Proceedings of the Institute of Acoustics

Noise Shaping and PWM for Power D/A Conversion

J.M. Goldberg and M.B. Sandler

Department of Electronic and Electrical Engineering, Kings's College, University of London

ABSTRACT

Results from simulations of the performance of new topologies for digital audio power amplifiers are presented. Digital pulse width modulation is used in conjunction with noise shaping techniques to convert digital audio data directly into analogue power. Simple second order systems are analysed with the aim of determining appropriate system parameters for the construction of a prototype.

1. Introduction

Although more and more of the audio recording/editing/playback process is performed digitally, very little work to date has been reported on the use of digital techniques for the *direct* conversion of digital audio data into analogue power.

Earlier work [1-3] has shown that pulse width modulation (PWM) may be suitable for digital power amplification with no intermediate digital-to-analogue conversion stage. (See Fig. 1.) Although, PWM is a highly non-linear process, increasing the sampling rate of the digital signal applied to a pulse width modulator's input significantly improves its linearity. Unfortunately, irrespective of oversampling, excessively high internal clock rates make an audio quality (i.e., 16 bit) pulse width modulator impractical.

This paper will demonstrate by simulation how the application of interpolative noise shaping techniques can help improve the linearity as well as the realizability of PWM for digital power amplification. We will begin with a general discussion of both PWM and noise shaping and will continue with descriptions and evaluations of the respective systems analysed.

2. PWM

PWM is a process whereby information-bearing signals are represented as variations in the width of high frequency pulses. In the past, so called "naturally sampled" PWM has been used to modulate analogue signals onto a high frequency pulse waveform as variations in the mark/space ratio. In essence, this may be done by applying the analogue signal to one input of a simple comparator and a high frequency triangle waveform to the other. The output of the comparator changes states such that naturally sampled PWM is produced.

In naturally sampled systems, the sampling instants are signal dependent. Since digital audio signals are sampled at regular, uniform instants of time, so called "uniformly sampled" PWM must be used. In this case, discrete time signals may be represented as variations in the width of *regularly occuring* high frequency discrete-width pulses. The circuit analogy for naturally sampled PWM may be adapted to obtain uniformly sampled PWM by simply passing the message signal through a sample and hold device operating at the triangle waveform's frequency before applying it to the comparator input. This is shown in Fig. 2.

For *digital* PWM, the comparator simply becomes a digital comparator and the comparison waveform is taken as the output of a counter. In these systems, the pulsewidths are distributed over a finite set of possible values (i.e., the waveform is quantized in the *time* domain). There is thus a minimum resolvable difference in pulseduration corresponding to one least significant bit in the digital signal representation. (These periods are the reciprocal of the final columns in Tables 1 and 2.)

With uniformly sampled PWM, we may chose to modulate one or both sides of the high frequency pulse as shown in Fig. 3. In either case, the spectra of uniformly sampled PWM tone modulation is such that the transmitted message and its harmonics are present in addition to the sampling frequency and its message sidebands along with their replicates. The only significant distortion terms present in the audio band are the harmonics of the message signal. In section 5, we will see how these levels of harmonic distortion are related to F_s, the sampling or "pulse repetition frequency" (i.e., the frequency of the triangle wave in the circuit analogy), f_o, the frequency of the message signal, and m is the modulation index or signal level of the message signal relative to full scale.

3. Interpolative Noise Shaping

After highlighting some of the theoretical and practical aspects of noise shaping, we will describe how such devices can be used in conjunction with PWM systems.

3.1. Background

Noise shaping is a technique whereby quantization noise is reduced by placing a feedback loop around a quantizer such that the quantization noise is frequency shaped. A simple noise shaping structure is shown in Fig. 4a. The lower order bits discarded by the quantizer (i.e., the quantization noise) are shaped by $H(z)$ before being fed back to the input.

For the purpose of analysis, it is often convenient (and reasonable in the case of high quality audio signals) to regard the quantizer as an additive noise source characterised by its z-Transform, $Q(z)$. The output of the noise shaper is then comprised of an unaltered version of the input signal in addition to a filtered version of the quantization noise as described by

$$Y(z) = X(z) + Q(z)[1 + H(z)] \tag{1}$$

with $Y(z)$ and $X(z)$ as the z-Transforms of the noise shaper output and input, respectively.

$H(z)$ should be chosen so as to create high loop gain at frequencies which are low compared to the sampling frequency. A set of "robust" filters whose coefficients are independent of signal and error statistics have been derived and are of the form

$$1 - H(z) = (1 - z^{-1})^N \tag{2}$$

where N is the filter order [4]. How well such a filter will attenuate in-band noise is independent of the input signal but does depend on the shape of the power spectral density of the noise. If we assume white quantization noise, the output error spectrum is such that low ($f_o << F_s$) frequency noise components will be much smaller than those at higher frequencies.

An "interpolative noise shaper" is a noise shaper preceded by a sample rate increase device. The increased bandwidth in the feedback loop makes it possible to attenuate quantization noise levels over the entire audio band which occupies only a fraction of the total bandwidth.

Thus for a given SNR specification, noise shaping permits a reduction in word length at the expense of circuitry operating at a higher sampling frequency. In general, for each doubling of the sampling frequency over the Nyquist minimum, $N+\frac{1}{2}$ bits may be dropped with no decrease in SNR. Fig. 4b shows this in terms of the reduction of in-band noise power for various ratios of sampling frequency, F_s, to signal bandwidth, F_b and filter orders.

As an illustration, Fig. 5 shows the output spectrum of a 16 bit 5KHz tone passed through a second order interpolative noise shaper operating at 705.6KHz with an 8 bit output. In-band noise attenuation and the steepness with which the noise floor rises against frequency increase with system order. However, stability problems in high order noise shapers of the topology shown in Fig. 4a restrict us to second order systems.

3.2. Implications for PWM

An interpolative noise shaper placed before a pulse width modulator as shown in Fig. 7c will have the effect of making the modulator more practical (by reducing its input word length) as well as making it more linear (by oversampling).

The modulator's internal clock rates for plain oversampled PWM are shown in Table 1 while the clock rates for interpolated noise shaped inputs are shown in Table 2. These rates refer to the speed at which the comparator logic within the modulator must operate. The combinations of noise shaper word length and sampling frequency have been chosen to give roughly the same effective SNR as 16 bit quantization with no oversampling. The rates displayed in Table 2 can easily be achieved with ECL technology.

Table 1: Internal Clock Rates for 16 Bit PWM (oversampled input)			
Modulation Type	b	F_s (KHz)	Clock Rate (GHz)
trailing edge	16	44.1	2.9
		352.8	23.1
		705.6	46.2
		1411.0	92.5
double sided symmetric	16	44.1	5.8
		352.8	46.2
		705.6	92.5
		1411.0	185.0

Table 2: Internal Clock Rates for b Bit PWM (oversampled, noise shaped input)			
Modulation Type	b	F_s (KHz)	Clock Rate (MHz)
trailing edge	13	352.8	2890.0
	8	705.6	180.6
	6	1411.0	90.3
double sided symmetric	13	352.8	5780.0
	8	705.6	361.3
	6	1411.0	180.6

4. Investigations

Fig. 6 shows the basic block diagram of the simulator. Since the signal generator is capable of producing tones at arbitrary sampling frequencies, the need for an interpolator is eliminated. The noise shaping module is a straight-forward second order (i.e., $N = 2$) implementation of the structure shown in Fig. 4. The pulse width modulator is capable of creating either trailing edge or double sided modulation of arbitrary word length. The decimator returns the sampling frequency to 44.1KHz, and the spectrum analyzer reveals the frequency domain characteristics of the PWM process by using FFT techniques in conjunction with a window possessing excellent side lobe behaviour. [5]

Simulations have been conducted to show the performance of trailing edge and symmetric double sided PWM with and without oversampling. Also, experiments have been performed with various second order interpolative noise shapers preceding both trailing edge and double sided pulse width modulators. The effects of varying the modulation index, signal frequency, and sampling frequency of the signals applied to the modulator are investigated as well. Fig. 7 shows the complete power amplifier block diagrams for each case. The low pass filter is used to remove high frequency spectral replicates before driving the loudspeakers.

5. Results

The output spectra of trailing edge and double sided symmetric pulse width modulators are shown in Figs. 8 and 9, respectively. The input signal is a full scale ($m \approx 1$) 16 bit, 1KHz tone with no oversampling (i.e., F_s = 44.1KHz). The distortion figures for trailing edge modulation are significantly higher than those for double sided symmetric modulation.

Figs. 10 and 11 show the effect of oversampling. Here an interpolator raises the sampling rate by a factor of 16. As expected the distortion has dramatically decreased.

Figs. 12 and 13 show the effect of a second order interpolative noise shaper driving trailing edge and double sided symmetric modulators. As before, the signal is oversampled by a factor of 16 but is then passed through a second order noise shaper which reduces the word length from 16 to 8 bits. Here the advantage of noise shaping becomes apparent. Comparing Figs. 10 and 11 and 12 and 13, respectively, show that if an interpolator is followed by an appropriate noise shaper, the PWM distortion levels are very similar. Thus, interpolative noise shaping offers PWM performance similar to plain interpolation but allows the modulator to process an input signal with a much smaller word length. As highlighted earlier in Tables 1 and 2, this implies manageable internal clock rates for the modulator. In this example, the modulator with an interpolated, noise shaped input may operate 256 times slower than the modulator with just an interpolated input.

The remaining experiments all use second order interpolative noise shapers and show the effect of varying the signal frequency, the modulation index, and the sampling frequency of the signal applied to the modulator. As double sided symmetric modulation offers consistently lower distortion, it will be the only modulation type considered from here onward.

Fig. 14a shows how, for a 1KHz full modulation input ($m = 1$), harmonic distortion levels fall with increasing F_s. With a 16X oversampled, 8 bit noise shaped input all the distortion terms are buried in quantization noise. Fig. 14b displays the distortion levels for a 5KHz full modulation input. The pattern is the same as in Fig. 14a, however increasing the signal frequency raises the distortion levels. Finally, Fig. 14c shows the effect of varying the modulation index, m, for a 16X oversampled, 8 bit noise shaped 5KHz input. (All distortion levels are relative to full scale.) The higher the modulation index, the higher the distortion levels.

The distortion levels in Fig. 14 are presented more to gain insight into the spectral characteristics of PWM in general. They must therefore be viewed in their proper "audio" context. As noted in [3], for audio signals, when signal frequency rises, signal level (i.e., the modulation index) falls dramatically such that these distortion effects tend to offset one another. As such, the higher level, higher frequency signal cases, which produce the worst distortion levels, are those which are least likely to occur with actual audio signals. For instance, 5KHz tones as high as 12dB beneath full scale can be modulated with all harmonic distortion small enough to be masked by quantization noise.

6. Conclusion

It has been shown that the application of interpolative, noise shaping techniques makes PWM a much more attractive method for digital power amplification. Specifically, interpolation makes PWM more linear and noise shaping makes PWM more practical. It has also been demonstrated that double sided symmetric modulation offers significantly better performance over trailing edge modulation at the expense of doubling the internal clock rate of the modulator.

Although the results presented are encouraging, there is much more to be done. Recently, new topologies for very stable higher order ($N > 2$) interpolative, noise shaping coders have been reported [6, 7] and research is currently underway to study the suitability of similar coders for digital power amplification. It is hoped that several prototypes incorporating second or higher order noise shaping modules will be operational in the near future.

7. References

[1] M.B. Sandler: "Towards a Digital Power Amplifier", presented at The 76th Convention of the Audio Engineering Society, 1984, New York, preprint no. 2135.

[2] M.B. Sandler: "Progress Towards a Digital Power Amplifier", presented at The 80th Convention of the Audio Engineering Society, 1986, Montreux, preprint no. 2361.

[3] M.B. Sandler: "Techniques for Digital Power Amplification", presented at Reproduced Sound 3, 1987, Windmere.

[4] S.K. Tewksbury and R.W. Hallock: "Oversampled, Linear Predictive and Noise-Shaping Coders of Order $N > 1$", IEEE Transactions on Circuits and Systems, Vol. CAS-25, No.7, July 1978.

[5] A.H. Nutall: "Some Windows with Very Good Sidelobe Behavior", IEEE Transactions on Acoustics, Speech, and Signal Processing, Vol. 29, No. 1, February 1981.

[6] K. Uchimura, T. Hayashi, T. Kimura, and A. Iwata: "Oversampled A-to-D and D-to-A Converters with Multistage Noise Shaping Modulators", IEEE Transactions on Acoustics, Speech, and Signal Processing, Vol. 36, No. 12, December 1988.

[7] W.L. Lee and C.G. Sodini: "A Topology for High Order Interpolative Coders", IEEE International Symposium on Circuits and Systems Digest, 1987.

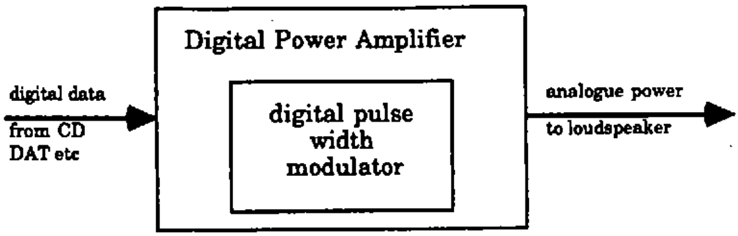

Fig. 1: Digital power amplification

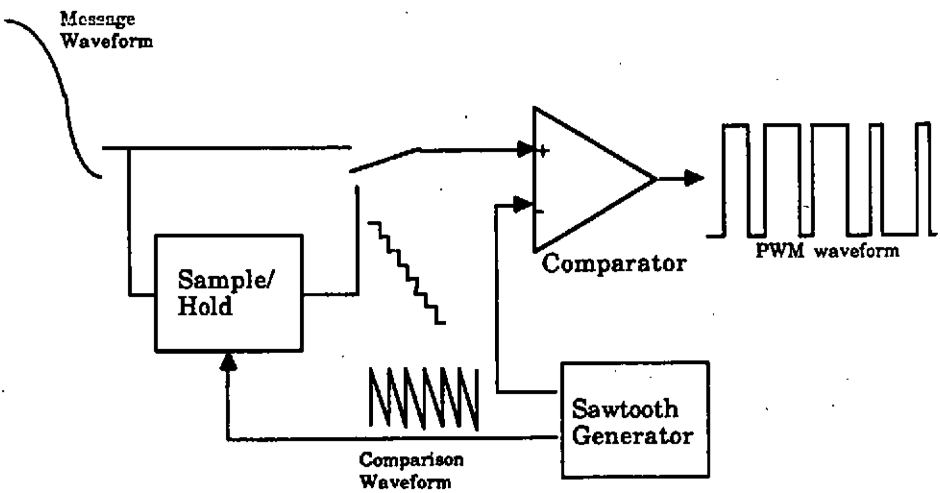

Fig. 2: Operation of Pulse Width Modulator

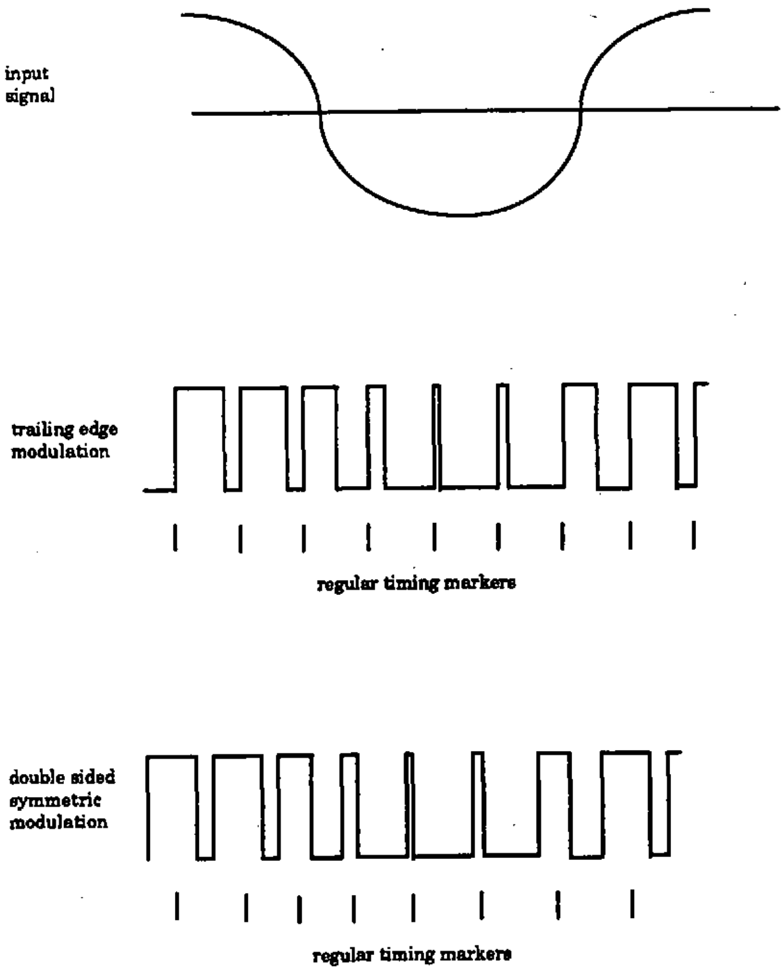

Fig. 3: Pulse Width Modulation Schemes

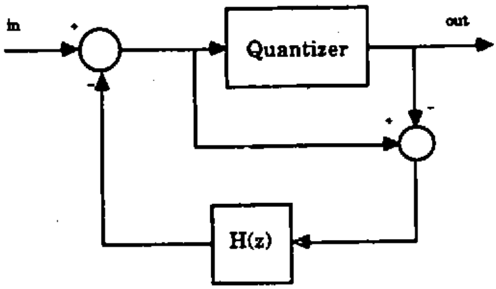

(a)

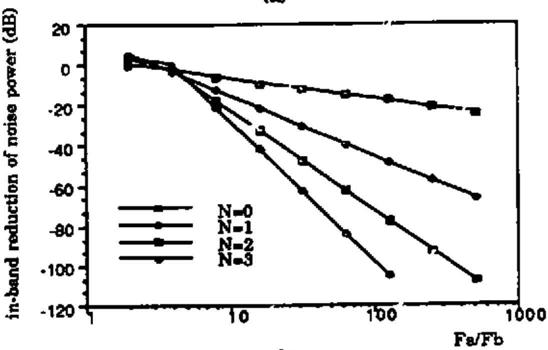

(b)

Fig. 4: (a) General Noise Shaper Topology
(b) Noise Power Reduction as a Function of Filter Order and Ratio of Sampling Frequency to Signal Bandwidth

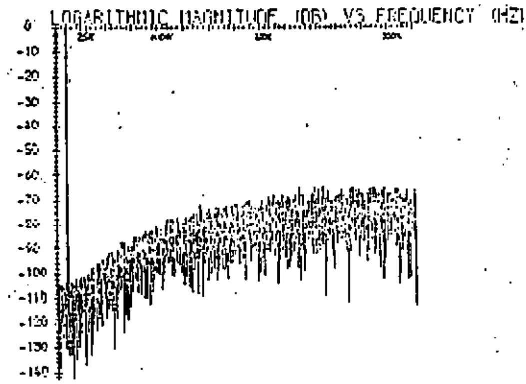

Fig. 5: Noise Shaper Output Spectrum

Fig. 6: The Simulator

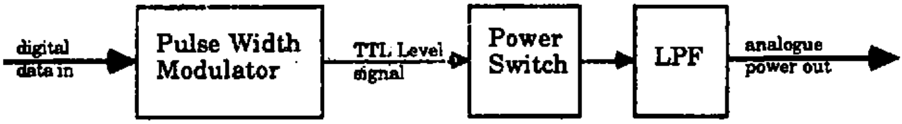

(a)

(b)

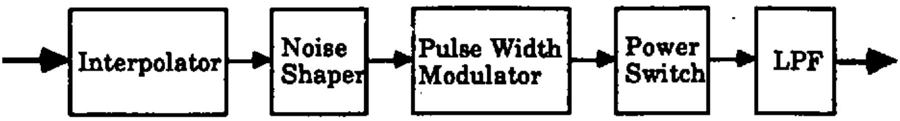

(c)

Fig. 7: Digital Power Amplifier Topologies

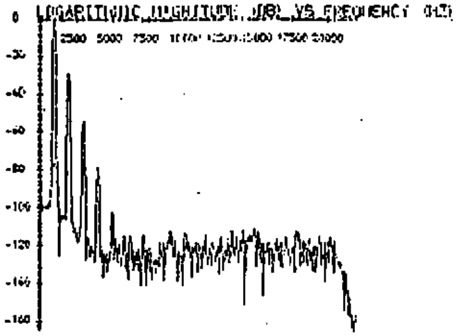

Fig. 8: Spectrum for trailing edge PWM (44.1KHz, 16 bit)

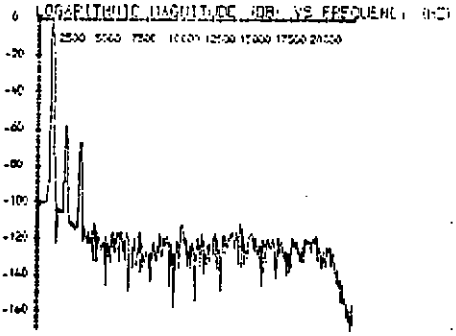

Fig. 9: Spectrum for symmetric double sided PWM (44.1KHz, 16 bit)

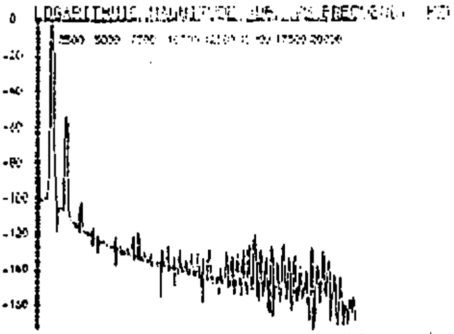

Fig. 10: Spectrum for trailing edge PWM (oversampled, 705.6KHz, 16 bit)

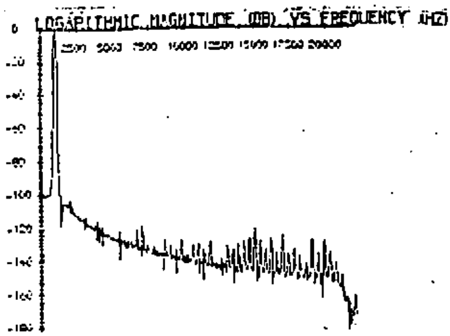

Fig. 11: Spectrum for double sided PWM (oversampled, 705.6KHz, 16 bit)

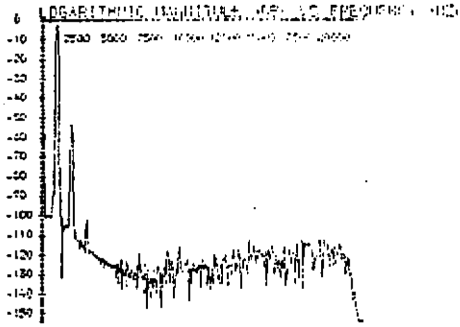

Fig. 12: Spectrum for trailing edge PWM (noise shaped, 705.6KHz, 8 bit)

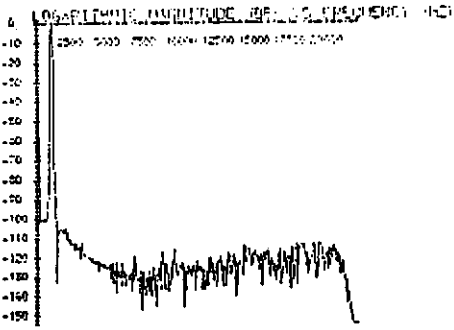

Fig. 13: Spectrum for double sided PWM (noise shaped, 705.6KHz, 8 bit)

Harmonic Distortion vs Fs
(double sided, 1KHz full scale input)

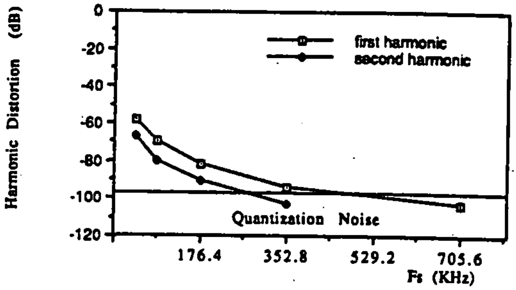

Fig. 14a

Harmonic Distortion vs Fs
(double sided, 5KHz full scale input)

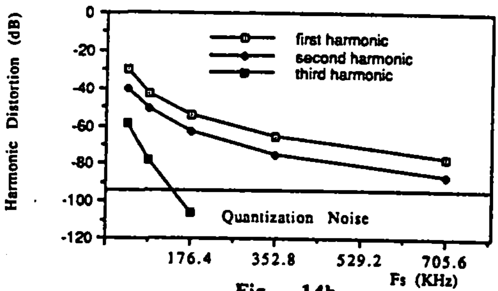

Fig. 14b

Harmonic Distortion vs m
(double sided, Fs = 705.6KHz, 5KHz input)

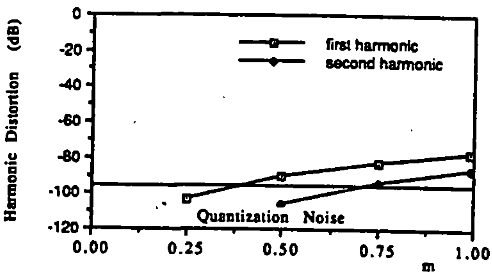

Fig. 14c